

Quantifying mRNA levels across tissue sections with 2D-RT-qPCR

Michael Armani · Michael A. Tangrea · Benjamin Shapiro · Michael R. Emmert-Buck · Elisabeth Smela

Received: 16 March 2011 / Revised: 23 April 2011 / Accepted: 25 April 2011 / Published online: 11 May 2011
© Springer-Verlag 2011

Abstract Measurement of mRNA levels across tissue samples facilitates an understanding of how genes function and what their roles are in disease. Quantifying low-abundance mRNA requires a workflow that preserves spatial information, isolates RNA, and performs reverse-transcriptase quantitative polymerase chain reaction (RT-qPCR). This is complex because these steps are typically performed in three separate platforms. In the present study, we describe two-dimensional RT-qPCR (2D-RT-qPCR), a method that quantifies RNA across tissues sections in a single integrated platform. The method uses the grid format of a multi-well plate to macrodissect tissue sections and preserve the spatial location of the RNA; this also eliminates the need for physical homogenization of the tissue. A new lysis and nucleic acid purification protocol is performed in the same multi-well plate, followed by RT-qPCR. The feasibility 2D-RT-qPCR was demonstrated on a variety of tissue types. Potential

applications of the technology as a high-throughput tissue analysis platform are discussed.

Keywords Tissue lysis · RNA purification · Gene expression mapping · Tissue section · PCR

Introduction

Measuring mRNA expression in different subregions of tissues is one approach towards understanding the biological role of genes. Techniques such as in situ hybridization (ISH) can visualize mRNA in histological sections, but ISH has generally poor sensitivity [1–6]. To address the need for better measurement capability, in situ PCR was invented in the early 1990s, combining the benefits of PCR amplification with subsequent in situ visualization [7]. Despite initial excitement over the technique, in situ PCR is generally too variable to consistently amplify desired targets within a complex tissue milieu [1–3, 8] and is most often used to detect high-abundance targets, such as viral DNA [9].

To quantify and localize moderate- and low-abundance nucleic acids investigators typically isolate tissue subregions and then perform PCR on each sample separately. For example, centimeter-scale regions of tissue are manually isolated using macrodissection [10, 11], or for slightly better resolution, tissue is cut into a millimeter scale grid using the voxelation method [12]. Laser-capture microdissection (LCM) is another technique for isolating subregions of a tissue section, but on a smaller length scale, including the recovery of individual cells [13–15]. Each of these approaches has provided useful information by integrating mRNA quantification with spatial information on the cellular source of the nucleic acids. However, all three are labor-intensive as each subregion of a histological section must be

Electronic supplementary material The online version of this article (doi:10.1007/s00216-011-5062-8) contains supplementary material, which is available to authorized users.

M. Armani · B. Shapiro
Fischell Department of Bio-Engineering, University of Maryland,
College Park, MD 20742, USA

E. Smela (✉)
Department of Mechanical Engineering, University of Maryland,
College Park, MD 20742, USA
e-mail: smela@umd.edu

M. Armani · M. A. Tangrea · M. R. Emmert-Buck (✉)
Pathogenetics Unit, Laboratory of Pathology,
National Cancer Institute,
Bethesda, MD 20892, USA
e-mail: buckm@mail.nih.gov

individually procured and processed using a four-step workflow that includes dissection, tissue homogenization and lysis, RNA purification, and reverse-transcriptase quantitative polymerase chain reaction (RT-qPCR). There are currently no protocols that integrate these four steps for studying mRNA from frozen tissue samples into a single-tube process.

We have previously demonstrated 2D-PCR [16], a method for mapping genomic DNA across a tissue section that integrates the desirable features of in situ measurements (spatial information) with the advantages of solution-based molecular analysis (sensitivity and quantitation). In 2D-PCR, the tissue section is transferred into a multi-well plate, using the grid format of the plate to mechanically subdivide the entire section into isolated regions. The tissue subregions are subsequently lysed in the wells, and the DNA is amplified while maintaining the spatial layout within the original tissue sample. In 2D-PCR, the steps of DNA extraction, PCR, and detection are performed on each tissue subregion using a single-well procedure.

Here we present 2D-RT-qPCR, a related technique that performs the more complex task of mapping and quantifying mRNA using a similar parallel-processing methodology; it includes RNA purification, reverse transcription, and qPCR (Fig. 1). To enable RNA extraction and purification in a plate format, we introduce a new single-well tissue lysis and RNA purification method using a chaotropic buffer and a solid-phase nucleic acid purification surface provided by ChargeSwitch magnetic beads. The 2D-RT-qPCR procedure is demonstrated by quantifying organ-specific and species-specific RNAs across a variety of tissue types.

Materials and methods

Quantitative PCR primers and probes

Multiplex PCR primers and hydrolysis probes for mouse GYS2, KCNJ1, and HPRT1 targets were generated using the Primer3 Web application, version 4.0 [17]. Primers and probes were obtained from Biosearch Technologies as described in the [Electronic Supplementary Material](#).

Tissue sections and scrapes

Frozen mouse liver, kidney, heart, brain and chicken thymus were obtained from Pel-Freez Biologicals. Individual organs and composites of multiple organs were embedded in O.C.T. Compound (Tissue-Tek) in a cryostat at $-24\text{ }^{\circ}\text{C}$. Tissues were sectioned to $10\text{ }\mu\text{m}$ thickness using a Leica cryostat microtome. Tissue scrapes were obtained by sectioning tissue onto glass slides, heating the slide at $90\text{ }^{\circ}\text{C}$ for 30 s, and scraping the dried tissue using a razor blade into 1.5 mL polypropylene tubes.

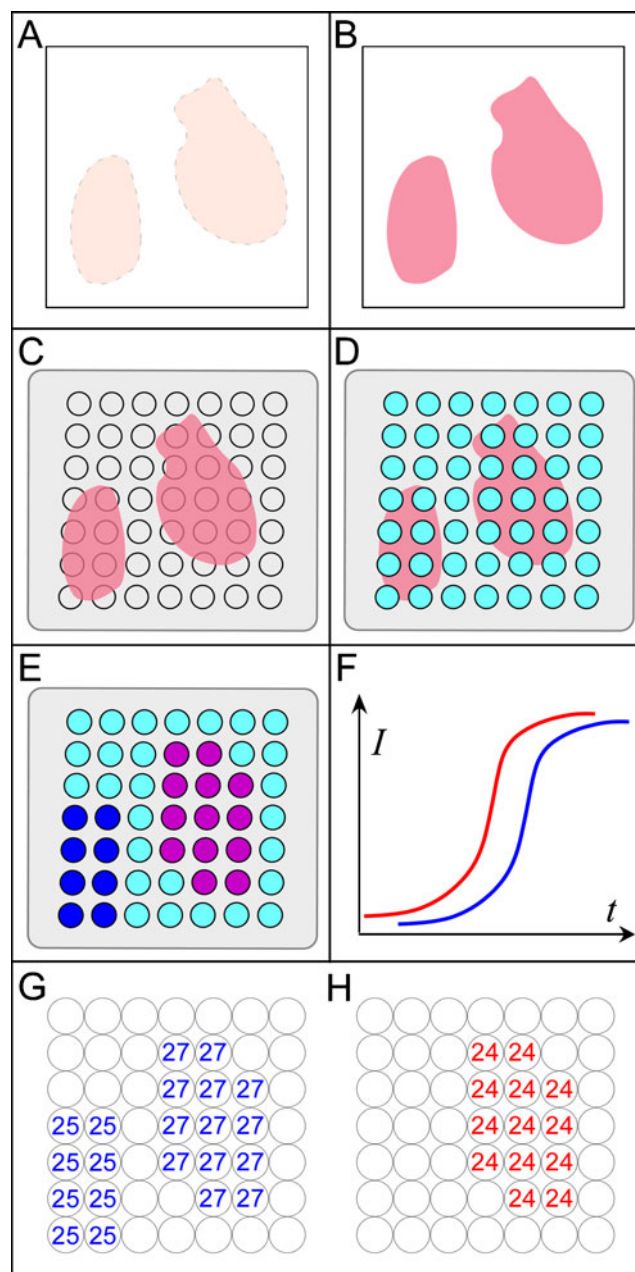


Fig. 1 Illustration of the 2D-RT-qPCR concept. **A** Tissues are sectioned onto adhesive film, **B** stained for visualization, and **C** transferred vertically onto a multi-well array device, which is **D** preloaded with cell lysis reagents. **E** RNA is extracted by chemical lysis, purified on capture beads, and **F** quantified by one-step multiplex reverse-transcriptase PCR in each well. **G** A housekeeping mRNA is quantified in each well for normalization and **H** one or more mRNA targets of interest are quantified

Materials and equipment

Heat-activated adhesive films were from Adhesives Research (ARSeal 90697). Industry standard 384-well transparent PCR plates were utilized (Applied Biosystems, 4309849). A Sorval RT7 swinging bucket was used to centrifuge these plates. In

place of a multiplexed 384-well real-time PCR instrument, plates were imaged using a fluorescent scanner every few cycles, and threshold cycles of detection (Cts) were determined as described in the [Electronic Supplementary Material](#).

Chemicals, buffers, kits, and reagents

A custom lysis buffer was prepared that contained 3.33 mL guanidinium isothiocyanate (GITC; 6 M, Fluka part 50983), 1.1 mL Triton X-100 (MPBio part 807426), 5 μ L 2-mercaptoethanol (Sigma part M3148), and 565 μ L double-distilled water. Buffer RLT was obtained from Qiagen (RNeasy kit). PicoPure Extraction Buffer and purification columns were obtained from Molecular Devices (PicoPure RNA Isolation kit). ChargeSwitch lysis buffer, magnetic beads (supplied in solution at 1 μ g/ μ L), wash buffers, and elution buffers were obtained from Invitrogen (ChargeSwitch total RNA cell kit 45–7006). The ChargeSwitch magnetic beads had a reported DNA binding capacity of 1 μ g/ μ L. The PicoPure columns had a reported maximum capacity of 100 μ g per column. Dried, sheared herring sperm DNA was obtained from Invitrogen (15634–017). Ag-Path ID one-step RT-PCR reagents were prepared according to the manufacturer's protocol (ABI, AM1005M), and 250 nM primers and 125 nM probes were included.

Determination of single-well purification protocol efficiency

Amounts of input and recovered DNA were measured in triplicate using a Nanodrop Spectrophotometer (Thermo-Scientific) using a test volume of 1 μ L. The efficiency was calculated as shown in Eq. 1:

$$\eta = \frac{DNA_{Out}}{DNA_{In} \bullet Volume_{Elution}} \bullet 100\% \quad (1)$$

2D-RT-qPCR

Method

The 2D-RT-qPCR procedure is illustrated in Fig. 2. (A) The tissue section is transferred onto an adhesive film, placed tissue-side down over a multi-well plate that has been preloaded with lysis buffer, and sealed. (B) The plate is inverted to distribute the lysis solution over the tissue, allowing sufficient incubation time to extract the RNA. (C) Magnetic ChargeSwitch beads are added to bind the nucleic acids in the lysate. (D) A magnet is brought close to the wells, attracting the beads and holding them in place for RNA purification, washing, and DNase treatment. (E) One-

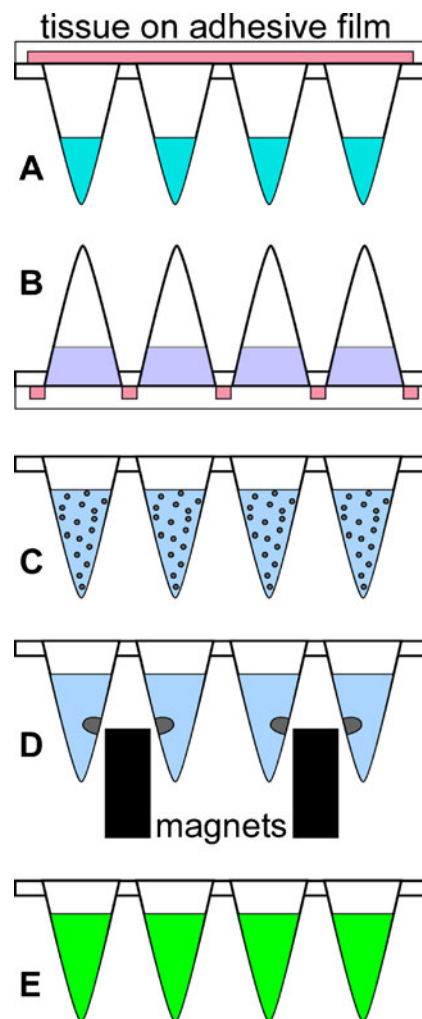


Fig. 2 Cross-sectional schematic illustration of the 2D-RT-qPCR method. **A** Tissue transfer onto a multi-well plate. **B** Tissue lysis. **C** Addition of magnetic capture beads. **D** Immobilization of beads and purification of RNA by washing and DNase treatment. **E** Amplification of RNA by RT-qPCR

step reverse-transcriptase PCR (RT-PCR) mix is added to the wells, and thermocycling with real-time detection is used to quantify the amounts of RNA transcript in each well. The procedure produces a quantitative map of mRNA at each well location, corresponding to the histological subregions of the original tissue section.

2D-RT-qPCR protocol for quantifying mRNA across tissue sections

The preferred protocol for performing 2D-RT-qPCR, developed using the data presented in the “[Results](#)” section, is given here. The steps correspond with those in Fig. 2.

A. Tissue transfer

Wells of a 384-well plate were loaded by pipette with 5 μ L of custom GITC lysis buffer (3.33 mL

GITC, 1.1 mL Triton X-100, 5 μ L 2-mercaptoethanol, and 565 μ L double-distilled water). Tissues were sectioned (“[Tissue sections and scrapes](#)”) and adhered to a 40 \times 40 mm piece of heat-activated adhesive film. The tissue sections were dried at 50 $^{\circ}$ C for 2 min, rinsed in a bath of 70% ethanol for 2 min (containing either 1% eosin Y or 1% acid fuchsin red stains for visualization) and placed at room temperature in a fume hood to speed up the drying process (10 min). The adhesive film with dried tissue was placed facedown onto the 384-well PCR plate. To seal the adhesive film against the plate, the adhesive was heat-activated at 90 $^{\circ}$ C for 5 min and compressed with 200 lbs (90 kg) of force [16]. After sealing, the plate was cooled at room temperature for 2 min.

B. Tissue lysis

To lyse the tissue overlying the wells, lysis buffer that had been previously loaded into the wells was distributed over the tissue by inverting the plate. To enhance the lysis, heat was applied to the tissue side of the plate using the flat surface of a heated 8-mm thick aluminum block placed on top of a standard 384-well thermocycler. A rubber pad was placed over the back of the plate, and the setup was compressed to prevent fluid from leaking. The contents of the wells were incubated for 15 min, applying 60 $^{\circ}$ C on the tissue side and, to prevent condensation, 70 $^{\circ}$ C on the back side. The plate was then cooled to 30 $^{\circ}$ C and centrifuged at 3,000 rpm for 3 min to move the lysate into the bottom of each well.

C. Nucleic acid isolation

To isolate the nucleic acids freed by lysis, an acidic buffer containing magnetic capture beads was added to the lysate in each well (0.33 μ L ChargeSwitch magnetic beads washed with water and dried, 0.4 μ L acetic acid, and 14.6 μ L water). The beads capture both RNA and DNA. To maintain an air space between the lysate and adhesive films, the maximum reagent volume in each well was 20 μ L (5 μ L for the GITC buffer and 15 μ L for water, beads, and acid).

D. Purifying the RNA

To purify the RNA, the magnetic beads were immobilized by a small cylindrical magnet placed between every other well, and the fluid removed by pipette. For the first rinse, ChargeSwitch wash buffer no. 13 (20 μ L) was added to each well and removed. To remove genomic DNA, ChargeSwitch DNase buffer (15 μ L) with DNase I (0.15 μ L) was added to each well and incubated for 10 min at room temperature; because of the low temperature, sealing was not required. ChargeSwitch binding buffer B9 (5 μ L) was added to each well, and the plate was sealed (ARseal 90697 at 90 $^{\circ}$ C for 1 min). The plate was inverted

several times to mix the contents, after which the plate was centrifuged as before. The DNase buffer was removed; two washes were performed using 20 μ L ChargeSwitch wash buffers no. 13 and no. 14, and the final wash buffer was removed. (Note: To use this procedure to isolate DNA from frozen tissues, the DNase step would be omitted.)

E. Reverse-transcriptase quantitative PCR

To quantify RNA across the multi-well plate, RT-qPCR reagents were added to each well and the plate was subjected to thermocycling and imaged every few cycles. Ag-Path ID one-step PCR mix was added to each well of the plate (7.5 μ L). Amplification was performed by thermocycling (50 $^{\circ}$ C for 15 min, 95 $^{\circ}$ C for 15 min, and 30 total cycles of 95 $^{\circ}$ C for 10 s and 60 $^{\circ}$ C for 30 s). The plate was imaged on a fluorescent microplate reader (Tecan 200) and threshold cycles of detection (Cts) were determined using a standard curve formula as described in the [Electronic Supplementary Material](#).

Results and discussion

The development and validation of 2D-RT-qPCR was done using 384-well plates and ChargeSwitch magnetic recovery beads in a well volume of 40 μ L. The use of such a small volume had not previously been reported, so the first step of the development was characterization of the purification efficiency, described in “[Efficient purification at small scales](#).” DNA was added into a mixture of ChargeSwitch lysis buffer, binding buffer, and beads, representing the contents of the wells during the isolation process (step C of the protocol). These experiments showed that the pH of this solution must be adjusted to maximize nucleic acid recovery in small volumes. The ChargeSwitch lysis buffer was, however, ineffective on tissue sections, requiring a change to a GITC-based buffer. “[GITC buffers in magnetic bead-based purifications](#)” describes the development of a custom GITC buffer with adjustments in pH and salinity that allowed DNA to be efficiently recovered. Using these developments, lysis and RNA recovery experiments were performed on tissue scrapes added into the wells, followed by RNA purification and amplification; this work is described in “[Single-well lysis and purification of tissue samples](#).” Observations coupled with RT-qPCR data for a normalizer (HPRT1) in three different mouse tissue types confirmed that the custom lysis buffer thoroughly lysed the tissue and also resulted in high recovery. Having completed the development of a protocol for 2D-RT-qPCR, proof of concept for the spatial mapping of RNA was demonstrated, as shown in “[Proof of concept for 2D-RT-PCR](#)” using a composite tissue section (comprising mouse brain, mouse kidney, and chicken thymus) mounted to a transfer

adhesive. Multiplex RT-qPCR was performed to produce maps of HPRT1 and KCNJ1 (found only in kidney). Another set of maps was produced to validate these results, described in “Validation of the optimal lysis buffer for 2D-RT-qPCR.”

Efficient purification at small scales

To perform 2D-RT-qPCR using 384-well plates, a lysis and purification protocol was required that would work at volumes of 40 μ L or less. The ChargeSwitch purification kit was chosen for the purification step since it utilizes magnetic beads and thus appeared to be scalable; however, ChargeSwitch reactions are typically based on 800 μ L volumes, so the feasibility of scaling down this protocol 20-fold was evaluated. Furthermore, because the ChargeSwitch protocol recommends pipette mixing (aspirating fluid in and out of a pipette multiple times) in each well, which would be too laborious across a 384-well plate, vortexing of magnetic beads was tested as an alternative. While vortexing is not required in the 2D-RT-qPCR protocol, for which the tissue sections are mounted onto adhesive tape, it is helpful when using tissue scrapes with the new single-well tissue lysis and RNA purification method. Under the assumption that the relative recovery efficiency of sheared DNA is similar to RNA, sheared DNA was selected as the input nucleic acid because it is close in size to RNA and is a stable and readily accessible reagent for systematic quantification.

Twenty-five microliters ChargeSwitch lysis buffer, 5 μ L of ChargeSwitch magnetic beads, and 10 μ L of ChargeSwitch binding buffer were added to individual 0.2 mL polypropylene tubes containing either 125 or 2,500 ng of dried sheared herring sperm DNA, corresponding to 2.5% and 50% of the

maximum capacity of the beads, respectively. After vortexing and waiting 1 min, each tube was placed over a magnet for 1 min to collect the beads and the lysis buffer removed. Vortexing and buffer removal were repeated with 40 μ L of ChargeSwitch wash buffer no. 13 and 40 μ L of ChargeSwitch wash buffer no. 14. Finally, 20 μ L of ChargeSwitch elution buffer was added to each well, and the plate was placed on ice after 2 min. To provide a point of reference, the unmodified ChargeSwitch protocol was followed according to the manufacturer’s instructions (using an 800 μ L volume). The efficiency of another purification kit, PicoPure, was also used as a comparator, following the manufacturer’s instructions. The loading was again set to 2.5% or 50% of the maximum binding capacity. Each experiment was performed at least three times to determine run-to-run variability. The amount of DNA recovered from each purification was measured to determine the nucleic acid recovery efficiency as described in “Determination of single-well purification protocol efficiency.” The results are shown in Table 1.

The ChargeSwitch (CS) protocol yielded more DNA than the PicoPure (PP) protocol, but, for both kits, recovery efficiencies were higher at 2.5% loading than at 50%. At 2.5%, the 20-fold scaled-down protocol provided similar purification efficiency (86%) as the unmodified CS protocol. At 50% loading, however, the recovery was only 30% for the scaled-down protocol vs. 47% for the standard method. In order to mitigate the loss of efficiency at higher loading, the addition of acetic acid (AA) was tested based on the fact that the magnetic beads require a pH of less than 6.0 to bind nucleic acids (according to the product manual) and an assumption that lower pH would increase the speed of nucleic acid binding. All three AA concentrations tested (1–4%)

Table 1 DNA recovery efficiency using two commercially available kits—ChargeSwitch Total RNA Cell Kit and PicoPure

Row	Kit	DNA% load	Max (μ g)	Recovery efficiency%	SD, %	<i>N</i>
1	PP	2.5	100	31	11	3
2	PP	50	100	8	3	3
3	CS	2.5	100	86	3	3
4	CS	50	100	47	7	3
5	CS/20	2.5	5	86	12	3
6	CS/20	50	5	30	4	6
7	CS/20+1% AA	50	5	50	3	3
8	CS/20+2% AA	50	5	38	1	3
9	CS/20+4% AA	50	5	37	2	3

Rows 1–4: comparison of DNA recovery efficiency using two commercially available kits: ChargeSwitch Total RNA Cell Kit and PicoPure. Rows 5–6: recovery efficiency of the scaled-down volume ChargeSwitch protocol (“CS/20”). Rows 7–9: the same protocol with the addition of acetic acid (AA).

DNA% load refers to the amount of DNA injected as a percentage of the maximum nucleic binding capacity of that kit; Max refers to total nucleic acid binding capacity of the purification method, and recovery efficiency is defined as $100\% \times \text{DNA}_{\text{out}} / (\text{DNA}_{\text{in}} \times \text{volume}_{\text{elution}})$.

CS ChargeSwitch, PP PicoPure, SD is the standard deviation, *N* is number of independent samples tested.

improved efficiency, with the 1% solution raising the efficiency the most, to 50%, similar to the standard protocol.

Overall, these data demonstrate that nucleic acid purification using ChargeSwitch magnetic beads can be performed in relatively small volumes without sacrificing efficiency by an appropriate adjustment of the pH. In contrast, the PicoPure protocol, which is based on the silica-purification method [18], had lower nucleic acid recovery and would be more difficult to scale down because of the number of tubes and centrifuge steps required.

GITC buffers in magnetic bead-based purifications

The experiments in “Efficient purification at small scales” showed that it is possible to scale down the ChargeSwitch purification. However, the lysis buffer supplied with the ChargeSwitch kit was not intended for digesting intact tissue, and, in initial testing, it did not fully lyse tissue components. The tissue remnants caused several difficulties: The magnetic beads flocculated unpredictably, pipette tips became clogged, and the beads could not be uniformly washed. Therefore, performing 2D-RT-qPCR using the mild denaturing ChargeSwitch lysis buffer would require painstaking pipette mixing to adequately re-suspend the beads and ensure a successful purification.

GITC-based lysis buffers are more aggressive and can disrupt intact tissue because GITC is a powerful chaotropic denaturant. Therefore, the compatibility of GITC lysis buffers with ChargeSwitch beads was evaluated using the same approach as in “Efficient purification at small scales.” Three GITC-based buffers were tested to determine their compatibility with CS magnetic beads: PicoPure buffer, Qiagen RLT buffer, and a custom buffer prepared in the laboratory (specified in “Chemicals, buffers, kits, and reagents”). Also, based on the results of “Efficient purification at small scales,” the addition of acetic acid was tested to assess the effects of a pH of 4.0.

Five microliters of ChargeSwitch magnetic bead solution was added to individual 0.2-mL polypropylene tubes; the beads were washed twice with double-distilled water, and 40 μ L of one of the GITC lysis buffers was added. Alternatively, a mixture of 39.2 μ L of GITC and 0.8 μ L acetic acid, a mixture of 10 μ L of GITC-based buffer and 30 μ L of water, or a mixture of 10 μ L of GITC-based buffer and 29.2 μ L of water with 0.8 μ L

acetic acid was added to the beads. For Qiagen RLT buffer, only 0.4 μ L of acetic acid was used. The GITC-bead mixtures were added to a second tube containing 2,500 ng of dried, sheared herring sperm DNA. The remaining steps of vortexing, washing, and elution were performed as described in “Efficient purification at small scales.”

As shown in the first column of Table 2, none of these buffers were compatible with recovery of DNA using magnetic beads, showing efficiencies of 0% to 5%. The concentration of GITC in commercial buffers is 4–8 M, but above 4 M, GITC is known to prevent hybridization of nucleic acids [19]. Measurement of the three GITC buffers showed them to be pH 5.5. Although this is below the required pH of 6.0 level for binding nucleic acids to ChargeSwitch beads, it was insufficient for rapid binding of nucleic acids. Therefore, the buffers were diluted and their pH adjusted to 4.0 with the addition of acetic acid. As shown in column 4, recovery efficiencies rose to between 8% and 31%. (Dilution alone gave efficiencies of 0–1%, while adjustment of pH alone gave efficiencies of 2% for the kit buffers and 19% for the custom buffer.) These data demonstrate the use of GITC-based lysis buffers with subsequent nucleic acid capture on ChargeSwitch beads, representing an important step towards a single-tube-based RT-qPCR process.

The purification efficiency using the custom GITC lysis buffer was improved to 68% by modifying the wash procedures. In one modification, 300% by volume ethanol was added to the lysis buffer (instead of the water and acetic acid in the last column of Table 2), giving an efficiency of 68%. In a second approach, the magnetic beads were kept in the elution buffer for a period of 48 h, also resulting in an efficiency of 68%. Even though the recovery efficiency was improved greater than twofold with these alternate approaches, they add the unnecessary risk of tissue fragment contamination or RNA hydrolysis. For example, the ethanol-based modification could bind undesired proteins from a tissue lysate, and the extended elution increases the likelihood of RNA degradation by hydrolysis in alkaline buffers. Because PCR is used for the detection step, a twofold improvement in recovery efficiency yields only a one-cycle improvement in detection, thus these improvements may not be worth the additional risk.

Table 2 Recovery efficiencies with sheared herring sperm DNA using GITC-based lysis buffers

GITC buffer	Without adjustments	+300% H ₂ O	Adjusted to pH 4.0	+300% H ₂ O and pH 4.0
PicoPure	1%	0%	2%	8%
Custom	0%	1%	19%	31%
Qiagen RLT	5%	1%	2%	30%

Single-well lysis and purification of tissue samples

The results in “GITC buffers in magnetic bead-based purifications” demonstrated that ChargeSwitch beads are able to purify DNA spiked into GITC-based buffers. To determine whether the lysis and purification procedures were effective for RNA recovery from tissue, frozen scrapes of different mouse tissues were lysed in four different buffers. This was followed by RNA purification with the addition of ChargeSwitch beads, water, and acid and subsequent detection of HPRT1 mRNA by RT-qPCR.

Four sets of tissue scrapes of mouse brain, liver, and kidney were prepared as described in “Tissue sections and scrapes” from serial recuts. The first set was placed in a solution of 200 μ L ChargeSwitch buffer prepared according to the manufacturer’s protocol by mixing ChargeSwitch lysis buffer as provided in the kit with proteinase K to a final concentration of 200 μ g/mL and dithiothreitol to a final concentration of 5 mM. The second, third, and fourth sets were placed in tubes containing 87.5 μ L of custom GITC buffers, Qiagen RLT buffers, or PicoPure lysis buffers. The samples were vortexed on the highest setting for 30 s (Daigger Vortex Genie 2) and incubated at 65 $^{\circ}$ C for 15 min.

In order to purify the released RNA, 100 μ L CS binding buffer and 50 μ L ChargeSwitch magnetic beads were added to the tubes after the lysis step, as well as an additional 50 μ L CS binding buffer and 59 μ L water to allow proper binding of the nucleic acids. Each tube was vortexed and placed over a magnet for 2 min, and the fluid was removed. The beads were washed with 350 μ L of CS wash buffer no. 14, and this buffer was removed. One hundred twenty-five microliters CS DNase buffer containing 1.25 μ L DNase was added. After a 10-min incubation at room temperature, 40 μ L CS binding buffer was added, and, after one additional minute, the buffers were removed. Two more wash steps were performed, the first with 350 μ L CS wash buffer no. 13 and the second with 350 μ L wash buffer no. 14. Finally, 60 μ L CS elution buffer was added to the beads.

Visual observations revealed that the ChargeSwitch magnetic purification beads clumped when mixed with tissue lysates prepared with either the ChargeSwitch or Qiagen RLT buffers. Undigested tissue was left in the wells, which clogged pipette tips. Tissue fragments can also obstruct purification surfaces, cause inconsistent RNA recovery, and inhibit reactions such as PCR [20]. Subsequent treatment with DNase followed by washing caused the beads to flocculate

and settle. By contrast, no clumping or flocculation occurred using the PicoPure or custom buffers, and no undigested tissue was observed. The improved lysis is attributed to the higher concentrations of surfactant in combination with the GITC. Based on the nucleic acid recovery efficiencies in Table 2, which were four times higher for the custom lysis buffer than the PicoPure buffer, the custom lysis buffer is the best for use with a single-well lysis and purification protocol, combining full lysis with good nucleic acid recovery.

To further validate and determine the overall effectiveness of the RNA extraction and purification, a sample of the RNA purified using each buffer and tissue was transferred into a standard 96-well plate, and the level of HPRT1 (a housekeeping mRNA) was quantified using a standard one-step RT-qPCR protocol. One-microliter samples of elution buffer were taken from each tube and added to Ag-Path ID one-step RT-PCR mix containing an HPRT1 probe set. Real-time detection and thermocycling were performed using an AB7500 instrument (50 $^{\circ}$ C for 10 min, 95 $^{\circ}$ C for 10 min, and 40 total cycles of 95 $^{\circ}$ C for 15 s and 60 $^{\circ}$ C for 45 s).

Table 3 shows the PCR cycle detection thresholds (Cts) of HPRT1 mRNA. Only one data point was collected per reaction, but since the standard deviation of the PCR reaction for HPRT1 is typically 0.2 Cts, general conclusions can still be drawn.

For brain tissue, all four buffers gave comparable Cts (approx. 29). For liver and kidney tissues, the Cts for the ChargeSwitch and custom GITC lysis buffers were basically unchanged (29–30), with these two having similar performance, but the Qiagen and PicoPure buffers had higher Cts (31–34), indicating lower recovery of HPRT1. These results confirm that the custom GITC buffer is the optimal lysis buffer, combining high mRNA recovery with complete tissue homogenization in a one-tube protocol.

Proof of concept for 2D-RT-PCR

The combination of immobilizing a flat tissue section onto adhesive tape with the single-well protocol for lysing, purifying, and amplifying nucleic acids enables transcript measurements across a tissue using the 2D-RT-qPCR approach. Steps A through E of the protocol were followed as described in “2D-RT-qPCR protocol for quantifying mRNA across tissue sections,” with minor variations as given in the [Electronic Supplementary Material](#). To

Table 3 Effectiveness of single-well lysis and purification for different tissue types determined by quantitative reverse-transcriptase PCR. The cycles of detection (Cts) for HPRT1 are shown

	Custom GITC buffer	Qiagen RLT	PicoPure	ChargeSwitch
Brain	29.1	28.4	29.0	29.0
Liver	30.5	32.8	33.8	30.0
Kidney	29.0	31.4	32.7	29.4

maintain an air space between the lysate and adhesive films, a reagent volume of 20 μ L was used in each well.

To demonstrate the mapping procedure, an mRNA of interest and a housekeeping mRNA were quantified across a tissue section, using a single block of frozen tissue that contained mouse brain, mouse kidney, and chicken thymus. In this experiment, the tissue was stained with eosin Y to allow visualization during transfer onto the plate. A multiplex PCR reaction was performed using primer and probe targets for *KCNJ1*, which is kidney-specific, and *HPRT1*, a housekeeping gene expressed in all mouse tissues. The empty wells between tissues served as no-sample controls, while the chicken thymus served as a non-targeted species control.

Figure 3 shows the composite tissue section on the plate (after step A), and the corresponding threshold cycles of detection (Cts) after RT-qPCR. *KCNJ1* mRNA was detected only in wells containing mouse kidney, and *HPRT1* was detected only in wells with mouse tissue. No false-positives were seen in any of the negative control wells. The *KCNJ1* primer/probe set amplifies both RNA and DNA; therefore, it is important to note that *KCNJ1* DNA was not detected in mouse brain even after 40 cycles of PCR, showing that the DNase treatment was effective and that only *KCNJ1* mRNA was amplified in the system. However, if the DNase step was omitted, *KCNJ1* was detected in all wells that contained mouse tissue ([Electronic Supplementary Materials](#)).

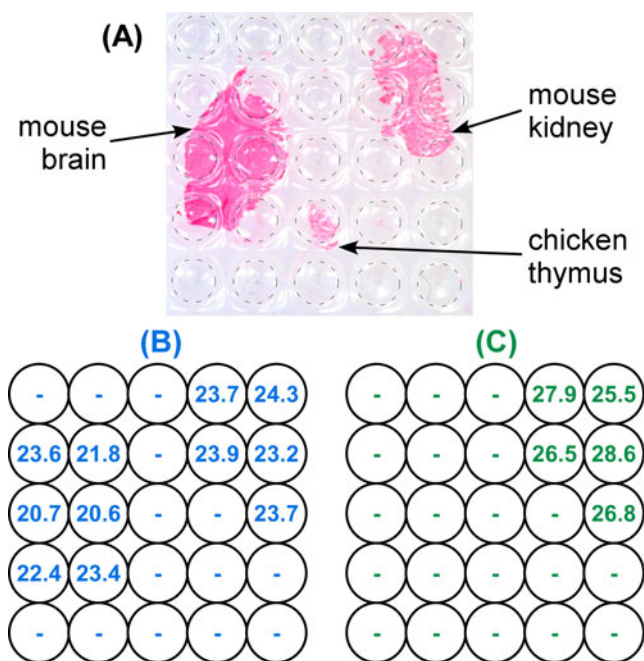


Fig. 3 **A** Photograph of a tissue section containing mouse brain, mouse kidney, and chicken thymus on an adhesive film, stained red with eosin Y and transferred onto a 384-well plate. The 384-well plate is visible under the tissue, and well positions are indicated by circular outlines. **B** *HPRT1* and **C** *KCNJ1* quantitative cycles of detection thresholds (Cts) determined by RT-qPCR at the well locations indicated in (A)

The fidelity of the map demonstrates that the wells were properly sealed during the initial lysis and that there was no cross-contamination during the procedure. In these tissues, the eosin Y stain was effectively removed during the purification steps, since there was no difference in fluorescence between wells that did and did not contain tissue. Overall, this experiment confirmed that it is possible to create a normalized map of a target mRNA in a tissue section using the 2D-RT-qPCR approach and of particular importance, that it is possible to detect *HPRT1*, a low-abundance mRNA, consistently across the sample.

Validation of the optimal lysis buffer for 2D-RT-qPCR

Lysis buffers were optimized in “Single-well lysis and purification of tissue samples” using tissue scrapes, which produce compacted tissue, loaded into the wells. In contrast, the 2D-RT-qPCR method begins with a single layer of thin tissue section that is transferred directly onto the plate. Therefore, to verify that the custom GITC buffer was more effective than the ChargeSwitch lysis buffer for 2D-RT-qPCR, the entire protocol was tested with both buffers by mapping mRNA in serial recuts of a composite tissue section containing mouse heart, kidney, and liver. A multiplex PCR reaction was performed using the same primer and probe targets as in “Proof of concept for 2D-RT-PCR” for *KCNJ1* and *HPRT1*. Another primer/probe set was added for *GYS2*, which is more highly expressed in liver than in other organs, with the aim of detecting a third multiplex target. The *GYS2* probe had a low quantum yield, giving weak signal amplification during PCR; therefore, tissue sections in these experiments were stained with acid fuchsin red for visualization because residual levels of fluorescent eosin interfered with quantitative PCR. A detailed protocol is given in the [Electronic Supplementary Material](#).

The effectiveness of each buffer for tissue lysis is shown in Fig. 4A. The custom GITC lysis buffer completely solubilized the three tissues (upper right panel), while the ChargeSwitch lysis buffer did not (upper left panel). The qPCR data shown in Fig. 4B–C further confirm this: on average, *KCNJ1* and *HPRT1* were detected 2.3 and 1.4 PCR cycles earlier when using the custom GITC buffer.

Again, as found previously with a different sample (Fig. 3), *HPRT1* was detected in all the wells containing mouse tissue, and *KCNJ1* was detected only in wells with kidney tissue. Also as expected, the greatest amount (lowest Cts) of *GYS2* was detected in liver, and the detection was consistent between serial recuts. However, multiplexing more than two colors is difficult without special optics, and it is expensive because it requires molecular beacons to give the required background suppression, critical for imaging multiple colors in the same well. Detecting more than two colors, even using a

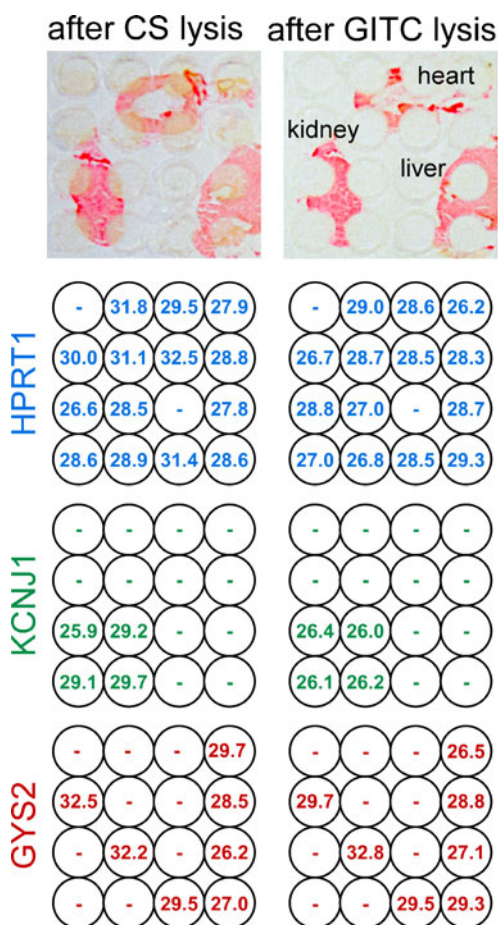


Fig 4 Two adjacent tissue sections (serial recuts) of a composite tissue block containing mouse heart, liver, and kidney, stained with acid fuchsin and transferred onto a 384-well plate containing either ChargeSwitch or custom buffer (image of tissue after lysis). **A** The layout of a 384-well format plate is outlined over the tissue. **B** KCNJ1 mRNA detection, **C** HPRT1 mRNA detection, and **D** GYS2 mRNA detection showing quantitative cycles of detection thresholds (Cts) determined by RT-qPCR

fluorescent plate reader, is challenging due to the dynamic changes in fluorescent signal during PCR, background noise, and signal crossover between color channels. This combination of primers and probes was not optimized to minimize background and prevent crosstalk between fluorescent channels, so it was not unexpected that the Cts in this experiment were not reliably quantitative for GYS2.

Discussion and conclusions

RNA recovery and detection from tissue specimens typically adheres to the following protocol: (1) dissection of the tissue, (2) physical grinding and homogenization in

lysis buffer followed by filtration of tissue fragments to prevent inconsistent RNA recovery, (3) RNA purification, and (4) PCR, together with the associated transfers of reagents between multiple tubes during these steps. This approach has proven to be labor-intensive and has thus posed a significant bottleneck for the study of nucleic acids from multiple tissue samples [21–24]. Multiple tubes can also lead to inconsistencies due to binding of nucleic acids to the tube walls or the purification column [21, 25, 26] and may increase the risk of cross-contamination between samples. In this study, the use of multiple tubes posed a major challenge for the development of 2D-RT-qPCR because these multi-tube workflows are difficult to integrate with histological tissue sections.

To increase the throughput of nucleic acid purification, the workflow complexity and labor requirements needed to be reduced. While this could have been done by robotic automation [21, 27] or using microfluidic sample processing chips [23, 28, 29], the approach described in this manuscript reduces the processing complexity by performing all the recovery steps in a single well using an aggressive buffer in place of physical homogenization. The “single-tube protocol” presented here was designed to eliminate the labor-intensive sample retrieval and transfer between tubes. Pipetting is only required for the addition of reagents and for the removal of fluid from the vials while the recovery beads are held firmly in place by a magnet, which can be done relatively easily and quickly. Using the described protocol, tissue from histological cryosections can be lysed completely with a GITC-based buffer and the RNA purified directly on ChargeSwitch magnetic beads. The protocol recovers mRNA as efficiently as commercially available systems and can be performed using small reagent volumes (the protocols were developed for 5 μ L of starting lysate).

Critically, the single-tube approach allows the use of an array format that maintains the original layout of nucleic acids during processing, so it enabled 2D-RT-qPCR. It should be noted, however, that parallel processing in a multi-well plate can also be used to increase throughput and consistency with a large number of different samples having no spatial relationships. For example, tissue blocks made from many archival specimens (tissue arrays) could be produced from small regions of tissue, sectioned once, and used directly with 2D-RT-qPCR. This will not only allow for higher throughput sample processing, but it will also reduce the waste of tissue when whole sections are not needed.

Immobilizing the tissue flat onto an adhesive tape eliminates folding and clumping of the tissue, resulting in a consistent lysis with no undissolved remnants in the well. The single-tube protocol can, however, also be performed on tissue scrapes, cell cultures, and, in principle, LCM samples.

The purpose of 2D-RT-qPCR is the quantification of target mRNAs corresponding to their original positions within the two-dimensional tissue architecture. After recovery, amplification is required to visualize moderate or low-abundant mRNAs. 2D-RT-qPCR therefore includes cell lysis, nucleic acid purification, and quantitative amplification in a single platform that maintains the spatial relationships. Proof of concept of 2D-RT-qPCR was demonstrated at the resolution of a 384-well plate by mapping two, and then three, mRNAs across a composite tissue section in a multiplex qPCR reaction. One of these was a housekeeping mRNA included to account for differences in the amount of material loaded into each well. The data presented in this paper suggest that 2D-RT-qPCR is robust with many tissue types. The capability of performing spatial mapping of mRNA levels across histological sections without the necessity of microdissection and separately running each sample, and without the necessity of adjusting the process for different types of tissue, is expected to facilitate studies on the function of genes and their potential roles in disease processes.

Increasing the resolution of the 2D-RT-qPCR system by decreasing the well size would allow for a broader range of molecular heterogeneity studies. A decrease in well size could be achieved by integrating the 2D-RT-PCR approach with existing microfluidic plates designed for high-throughput PCR, such as the Biotrove system [30], which uses 300- μm -sized wells. However, new challenges are introduced as the size of the wells shrinks, including an increase in surface adsorption of nucleic acids and PCR enzymes, an increase in the evaporation rate of the solutions, and a decrease in the amount of starting template per well. Increasing resolution is a current topic of our research.

The 2D-RT-qPCR data showed that multiplexing to multiple colored targets is, in principle, possible, although doing so requires careful optimization of the probes. However, while multiplexed RT-qPCR is fundamentally limited to detection of only a few mRNAs, this is not a limitation of the 2D-RT-qPCR technique. By converting the DNA or RNA to pre-amplified DNA or cDNA using 2D-RT-qPCR, each sample well can provide sufficient amplified product to allow dozens of subsequent PCR reactions, despite the small amount of tissue in each well. Using multiplex tandem PCR [31–33], it has previously been shown that up to 92 mRNAs can be studied from a single sample of purified mRNA, thus increasing the number that can be studied across a tissue section. Tandem PCR should be compatible with the 2D-RT-qPCR approach. Each of the pre-amplified targets can then be studied using existing primer/probe sets and single-plex real-time PCR machines with minimal optimization. This opens the door to using 2D-RT-qPCR to study dozens of mRNAs in a single tissue section. Other techniques could also be adapted for detection of the pre-amplified DNA, such as Fluidigm [34], Nanostring [35], microarrays [36], or

sequencing, to improve the number of nucleic acids studied. For all of these processes, the RNA or DNA targets would be pre-amplified by tandem PCR performed in the 2D-RT-qPCR wells. The pre-amplified targets would then be provided to the detection system according to standard protocols.

2D-RT-PCR is expected to complement methods such as LCM and in situ hybridization for discovering and validating the expression of mRNA in tissues. Correlation of quantitative mRNA levels with traditional histopathological techniques should lead to a greater understanding of the biological and pathological roles of mRNA and the discovery of important spatially dependent gene expression signatures. 2D-RT-PCR can be used in place of current voxelation [12, 37, 38] and macrodissection approaches to mapping RNA in histological sections and will likely have increasing utility as resolution is improved through miniaturization to a sub-millimeter scale.

Acknowledgments We would like to thank Connie Rogers-Newcome at Adhesives Research for providing samples of ARseal 90697 sealing films.

Funding This work was supported in part by the Intramural Research Program of the NIH, National Cancer Institute, Center for Cancer Research.

References

1. Nuovo GJ (1994) PCR in-situ hybridization. *Meth Mol Biol* 33:223–241
2. Long AA, Komminoth P (1996) In situ PCR. *Meth Mol Biol* 71:141–161
3. O’Leary JJ, Chetty R, Graham AK, McGee JOD (1996) In situ PCR: pathologist’s dream or nightmare? *J Pathol* 178:11–20
4. Dowsett M, Bartlett J, Ellis IO, Salter J, Hills M, Mallon E, Watters AD, Cooke T, Paish C, Wencyk PM, Pinder SE (2003) Correlation between immunohistochemistry (HercepTest) and fluorescence in situ hybridization (FISH) for HER-2 in 426 breast carcinomas from 37 centres. *J Pathol* 4:418–423
5. Hubbard RA (2003) Human papillomavirus testing methods. *Arch Pathol Lab Med* 127:940–945
6. Arvey A, Hermann A, Hsia CC, Le E, Freund Y, McGinnis W (2010) Minimizing off-target signals in RNA fluorescent in situ hybridization. *Nucleic Acids Res* 38:e115
7. Haase AT, Retzel EF, Staskus KA (1990) Amplification and detection of lentiviral DNA inside cells. *Proc Natl Acad Sci USA* 87:4971–4975
8. Bicknell GR, Shaw JA, Pringle JH, Furness PN (1996) Amplification of specific mRNA from a single human renal glomerulus, with an approach to the separation of epithelial cell mRNA. *J Pathol* 180:188–193
9. Heng B, Glenn WK, Ye Y, Tran B, Delprado W, Lutze-Mann L, Whitaker NJ, Lawson JS (2009) Human papilloma virus is associated with breast cancer. *Br J Cancer* 101:1345–1350
10. Paik S, Shak S, Tang G, Kim C, Baker J, Cronin M, Baehner FL, Walker MG, Watson D, Park T, Hiller W, Fisher ER, Wickerham DL, Bryant J, Wolmark N (2004) A multigene assay to predict recurrence of Tamoxifen-treated, node-negative breast cancer. *New Engl J Med* 351:2817–2826

11. Celotti F, Melcangi RC, Negri-Cesi P, Ballabio M, Martini L (1987) Differential distribution of the 5-alpha-reductase in the central nervous system of the rat and the mouse: are the white matter structures of the brain target tissue for testosterone action? *J Steroid Biochem* 26:125–129
12. Singh RP, Brown VM, Chaudhari A, Khan AH, Ossadtchi A, Sforza DM, Meadors AK, Cherry SR, Leahy RM, Smith DJ (2003) High-resolution voxelation mapping of human and rodent brain gene expression. *J Neurosci Methods* 30:93–101
13. Emmert-Buck MR, Bonner RF, Smith PD, Chuaqui RF, Zhuang ZP, Goldstein SR, Weiss RA, Liotta LA (1996) Laser capture microdissection. *Science* 274:998–1001
14. Rodriguez-Canales J, Hanson JC, Tangrea MA, Erickson HS, Albert PS, Wallis BS, Richardson AM, Pinto PA, Linehan WM, Gillespie JW (2007) Identification of a unique epigenetic sub-microenvironment in prostate cancer. *J Pathol* 211:410–419
15. Giannakis M, Stappenbeck TS, Mills JC, Leip DG, Lovett M, Clifton SW, Ippolito JE, Glasscock JI, Arumugam M, Brent MR, Gordon JI (2006) Molecular properties of adult mouse gastric and intestinal epithelial progenitors in their niches. *J Biol Chem* 281:11292–11300
16. Armani M, Rodriguez-Canales J, Gillespie J, Tangrea M, Erickson H, Emmert-Buck MR, Shapiro B, Smela E (2009) 2D-PCR: a method of mapping DNA in tissue sections. *Lab Chip* 9:3526–3534
17. Rozen S, Skaletsky H (2000) Primer3 on the WWW for general users and for biologist programmers. *Methods Mol Biol* 132:365–386
18. Boom R, Sol CJA, Salimans MMM, Jansen CL, Wertheim-Van Dillen PME, Van Der Noordaa J (1990) Rapid and simple method for purification of nucleic acids. *J Clin Microbiol* 28:495–503
19. Thompson J, Gillespie D (1987) Molecular hybridization with RNA probes in concentrated solutions of guanidine thiocyanate. *Anal Biochem* 163:281–291
20. Rådström P, Knutsson R, Wolffs P, Lövenklev M, Löfström C (2004) Pre-PCR processing: strategies to generate PCR-compatible samples. *Mol Biotechnol* 26:133–146
21. Bustin SA (2002) Quantification of mRNA using real-time reverse transcription PCR (RT-PCR): trends and problems. *J Mol Endocrinol* 29:23–39
22. Klebe RJ, Grant GM, Grant AM, Garcia MA, Giambernardi TA, Taylor GP (1996) RT-PCR without RNA isolation. *Biotechniques* 21:1094–1100
23. Tian H, Hühmer AFR, Landers JP (2000) Evaluation of silica resins for direct and efficient extraction of DNA from complex biological matrices in a miniaturized format. *Anal Biochem* 283:175–191
24. Giordano BC, Ferrance J, Swedberg S, Hühmer AF, Landers JP (2001) Polymerase chain reaction in polymeric microchips: DNA amplification in less than 240 seconds. *Anal Biochem* 291:124
25. Kamme F, Zhu J, Luo L, Yu J, Tran D, Meurers B, Bittner A, Westlund K, Carlton S, Wan J (2004) Single-cell laser-capture microdissection and RNA amplification. *Methods Mol Med* 99:215–223
26. To MD, Done SJ, Redston M, Andrusis IL (1998) Analysis of mRNA from microdissected frozen tissue sections without RNA isolation. *ASIP* 153:47–51
27. Obata K, Segawa O, Yakabe M, Ishida Y, Kuroita T, Ikeda K, Kawakami B, Kawamura Y, Yohda M, Matsunaga T, Tajima H (2001) Development of a novel method for operating magnetic particles, Magtration Technology, and its use for automating nucleic acid purification. *J Biosci Bioeng* 91:500
28. Zhong JF, Chen Y, Marcus JS, Scherer A, Quake SR, Taylor CR, Weiner LP (2008) A microfluidic processor for gene expression profiling of single human embryonic stem cells. *Lab Chip* 8:68–74
29. Hong JW, Studer V, Hang G, Anderson WF, Quake SR (2004) A nanoliter-scale nucleic acid processor with parallel architecture. *Nat Biotechnol* 22:435
30. Brenan CJH, Morrison T, Stone K, Heitner T, Katz A, Kanigan TS, Hess R, Kwon SJ, Jung HC, Pan JG (2002) Massively parallel microfluidics platform for storage and ultra-high-throughput screening. *SPIE* 4626:560
31. Stanley KK, Szewczuk E (2005) Multiplexed tandem PCR: gene profiling from small amounts of RNA using SYBR green detection. *Nucleic Acids Res* 33:e180
32. Li J, Smyth P, Cahill S, Denning K, Flavin R, Aherne S, Pirodda M, Guenther SM, O'Leary JJ, Sheils O (2008) Improved RNA quality and TaqMan® pre-amplification method (PreAmp) to enhance expression analysis from formalin fixed paraffin embedded (FFPE) materials. *BMC Biotechnol* 6:10
33. Cronin M, Pho M, Dutta D, Stephans JC, Shak S, Kiefer MC, Esteban JM, Baker JB (2004) Measurement of gene expression in archival paraffin-embedded tissues. *Am J Pathol* 164:35–42
34. Spurgeon SL, Jones RC, Ramakrishnan R (2008) High throughput gene expression measurement with real time PCR in a microfluidic dynamic array. *PLoS ONE* 3:e1662
35. Geiss GK, Bumgarner RE, Birditt B, Dahl T, Dowidar N, Dunaway DL, Fell HP, Ferree S, George RD, Grogan T, James JJ, Maysuria M, Mitton JD, Oliveri P, Osborn JL, Peng T, Ratcliffe AL, Webster PJ, Davidson EH, Hood L, Dimitrov K (2008) Direct multiplexed measurement of gene expression with color-coded probe pairs. *Nat Biotechnol* 26:317–325
36. Schena M, Shalon D, Davis RW, Brown PO (1995) Quantitative monitoring of gene-expression patterns with a complementary-DNA microarray. *Science* 270:467–470
37. Singh RP, Desmond JS (2003) Genome scale mapping of brain gene expression. *Biol Psychiatry* 53:1069–1074
38. Brown VM, Ossadtchi A, Khan AH, Cherry SR, Leahy RM, Smith DJ (2002) High-throughput imaging of brain gene expression. *Genome Res* 12:244–254

Analytical and Bioanalytical Chemistry

Electronic Supplementary Material

**Quantifying mRNA Levels Across a Histological Section
with 2D-RT-qPCR**

Michael Armani, Michael A. Tangrea, Benjamin Shapiro,
Michael R. Emmert-Buck, and Elisabeth Smela*

Primer Sequences Used in This Study

Table S1. Primer sequences

Primer sets (Biosearch Technologies)

Target	Gene annotation	Forward (5' to 3')	Reverse (5' to 3')
Mouse Liver GYS2	<u>NM_145572</u>	GCCAGACACCTGACACTGA	TCCGTCGTTGGTGGTGATG
Mouse Kidney KCNJ1	<u>NM_019659</u>	GGCGGGAAGACTCTGGTTA	GTGCCAGGAACCAAACCTA
Mouse Control HPRT1	<u>NM_013556</u>	GCAAACCTTTCCTTCCCTGG	ACTTCGAGAGGTCTTTTCACC
Target	Probe (5' to 3')		
Mouse Liver GYS2	5'CalFluorOrange560-TTCCAGACAAATTCCACCTAGAGCCC-BHQ1		
Mouse Kidney KCNJ1	5-FAM-AAGCACCGTGGCTGATCTTCCAGA-BHQ1		
Mouse Control HPRT1	5'Quasar670-CAGCCCCAAAATGGTTAAGGTTGCAAG-BHQ2		

The GYS2 and KCNJ1 primer and probe sets target both DNA and RNA with amplicon sizes of 73 and 67 bases. The HPRT1 target is intron spanning and only amplifies RNA efficiently with an amplicon size of 85 bases.

Specific Protocol for Duplex mRNA Mapping (ChargeSwitch Buffer)

The workflow outlined in section 3.2 of the manuscript was followed with a few modifications. First, a tissue section containing mouse kidney, mouse brain, and chicken thymus was sectioned on adhesive film and treated with eosin Y stain as described. This tissue on adhesive film was then thawed at 90 °C for 15 minutes, and transferred onto part of a 384-well plate – a 6x5 grid of wells – pre-loaded with ChargeSwitch lysis buffer. The film was sealed for 2 minutes total time. The fluid was distributed over the tissue by manually inverting the plate 5 times (instead of inverting the plate once). After lysis, ChargeSwitch beads and binding buffer were added to each well (0.33 µL ChargeSwitch magnetic beads, 0.4 µL acetic acid, 5.75 µL ChargeSwitch binding buffer, and 8.52 µL water). A wash was performed using 12.5 µL of wash #14, 6.25 µL of DNase was added and incubated for 10 minutes, and 2 µL of ChargeSwitch binding buffer (B9) was added. After removing the DNase buffers, two washes were performed using 20 µL of wash #13 and 12.5 µL of wash #14 buffers.

AgPath-ID one-step RT-PCR mix was prepared according to the manufacturer's protocol. The mix included final concentrations of 250 nM primers and 125 nM probes for both HPRT1 and KCNJ1 targets. Five µL of the PCR mix was added to each well in the 6x5 grid of wells. The thermocycling parameters were 50 °C for 10 minutes, 95 °C for 10 minutes, and 30 total cycles of 95 °C for 15 seconds and 60 °C for 30 seconds. The plate was removed and imaged on a Typhoon 1410 flatbed scanner every 5 cycles from cycles 15 to 30.

Specific Protocol for Triplex mRNA Mapping (ChargeSwitch or Custom GITC Buffer)

The workflow outlined in section section 3.2 of the manuscript was followed with a few modifications. Two 5x5 grids within a 384-well plate were pre-loaded with lysis buffer. In one grid, each well was preloaded with a mixture containing 12.5 µL ChargeSwitch lysis buffer, 6.25 µL binding buffer, 0.5 µL beads, 0.2 mg/mL proteinase K, 5 mM DTT, and acetic acid to a final

concentration of 2% by volume. In the second grid, each well was preloaded with 5 μ L of custom GITC-based lysis buffer. Two serial recuts of tissue containing mouse liver, kidney, and heart were made as described, stained red using acid fuchsin red, and placed on the two grids. The plate was inverted, incubated, centrifuged, and washed as described. AgPath-ID one-step RT-PCR mix was prepared according to the manufacturer's protocol, with final concentrations of 250 nM primers and 125 nM probes for each of the three targets, HPRT1, GYS2, and KCNJ1. The plate was removed and imaged at cycles 10, 25, 28, 31, 34, 37, and 40 using a Tecan 200 plate reader.

Example of 2D-RT-PCR Without DNase Treatment

A workflow similar to the one outlined in section 4.5 of the manuscript was followed for triplex mRNA mapping, but with the DNase step omitted. Again, as in Figure 4 of the manuscript, all the wells that had tissue showed a signal (Figure S1) from the HPRT1 housekeeper expressed in all mouse tissues. However, in addition, fluorescent data in all the wells with tissue also showed signals for KCNJ1 and GYS2 targets, which were not intron-spanning and could therefore detect genomic DNA. Comparing this detection map with the ones in Figures 3 and 4 of the manuscript showing KCNJ1 signals only in kidney tissue, it is apparent that DNase treatment is sufficient and necessary to provide a detection map specific to mRNA.

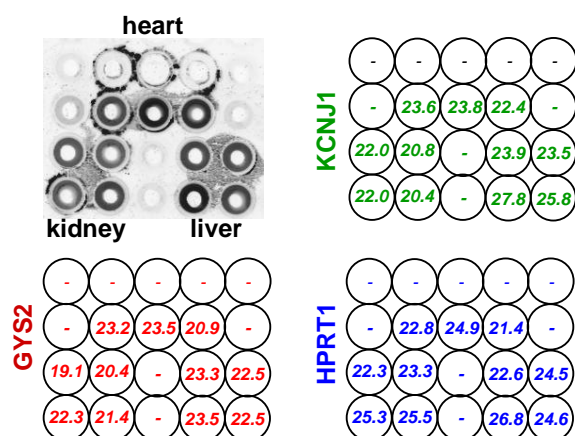


Figure S1. Fluorescent image showing the position of a mouse tissue section containing heart, liver, and kidney, and tissue lysate within wells. The fluorescence is provided by eosin Y staining of the tissue. Dark color within wells indicates that tissue was present and lysed. Three detection maps were obtained using 2D-RT-qPCR without DNase treatment. The results show the detection of GYS2, KCNJ1, and HPRT1 in all of the wells that contained tissue.

Fluorescent Data and Determination of Cts

It was necessary to perform PCR in a 384-well thermocycler, but a fluorescent plate reader was used to collect multiplex fluorescent data. Initially, a typhoon 1410 flatbed scanner was used to collect data at PCR cycles 15, 20, 25, and 30. However, a Tecan 200 plate reader was identified as a faster imaging system and was later used to measure fluorescence values. When using the Tecan to measure fluorescence for the KCNJ1, GYS2, and HPRT targets, excitation/emission wavelengths of 495/532, 538/573, and 649/679 nm were used. Because the Tecan instrument was faster,

fluorescence signal data could be obtained more frequently. Data was obtained at PCR cycles 10, 25, 28, 31, 34, 37, and 40.

In order to determine Cts, the difference between two cycles was calculated as $D_i = \log(\text{data}_{\text{cycle}(i)} / \text{data}_{\text{cycle}(i-1)})$, based on the standard curve formula of PCR (38). The cycle C_i was determined when D_i was greater than a threshold value; thresholds were defined as 0.04 for KCNJ1, 0.06 for GYS2, and 0.08 for HPRT1 to filter out background fluorescence. Finally, the Ct value was calculated as $C_i - A * D_i / 0.2$ for KCNJ1 and GYS2 or $C_i - A * D_i / 0.25$ for HPRT1. The constant value A was defined as the number of PCR cycles between fluorescent images (3 or 5). Based on negative controls and background values, Cts above 30.0, 32.5, and 35.0 were ignored for KCNJ1, HPRT1, and GYS2, respectively.

Binding of DNA to Adhesives Film

An experiment was performed to determine if nucleic acids could be adsorbed onto the adhesive films used in 2D-RT-qPCR due to the application of heat. It was assumed that DNA would bind in a similar way to RNA. Thus, 5000 ng of FAM (fluorescent) labeled DNA oligonucleotides were added to custom lysis buffer, which was added into three wells of a 384-well plate. The plate was inverted to bring the buffer into contact with the adhesive film and 60 °C heat was applied for 15 minutes. Using a second sample, the plate was inverted but no heat was applied. The two plates were centrifuged to pull the buffer back into the wells. The adhesive films were dried and then imaged using a fluorescent scanner. Using a dilution series of known amounts of dried labeled oligo as a comparison, it was determined that 2% or less of the DNA was bound to the adhesive films as a result of heating. Non-specific adsorption of DNA to surfaces is a known phenomenon and a major concern. However, the application of strongly denaturing buffer used in these experiments is expected to prevent most of the DNA from binding to the film, as was demonstrated in this experiment.